

# Fluid-Structure Interaction for Coolant Flow in Research-type Nuclear Reactors

**Abstract** The High Flux Isotope Reactor (HFIR), located at the Oak Ridge National Laboratory (ORNL), is scheduled to undergo a conversion of the fuel used and this proposed change requires an extensive analysis of the flow through the reactor core. The core consists of 540 very thin and long fuel plates through which the coolant (water) flows at a very high rate. Therefore, the design and the flow conditions make the plates prone to dynamic and static deflections, which may result in flow blockage and structural failure which in turn may cause core damage. To investigate the coolant flow between fuel plates and associated structural deflections, the Fluid-Structure Interaction (FSI) module in COMSOL will be used. Flow induced flutter and static deflections will be examined. To verify the FSI module, a test case of a cylinder in cross-flow, with vortex induced vibrations was performed and validated.

**Keywords** fluid flow, structural dynamics, fluid-structure interactions, FSI, COMSOL

---

## 1 Introduction

As the HFIR goes through the changes in fuel design from high-enriched uranium (HEU) to low-enriched uranium (LEU) fuel, the characteristics of the fuel plates are expected to change. The HEU is dispersion-type fuel (powder-based), whereas the LEU is a pure metallic structure; therefore, it is expected that the overall plate will be stiffer. Dur-

---

Research funded by the Department of Energy (DOE) Office of Science and the Global Threat Reduction Initiative (GTRI) of the National Nuclear Security Administration (NNSA) <http://nnsa.energy.gov/>

---

<sup>1</sup>Mechanical, Aerospace and Biomedical Engineering Dept. The University of Tennessee  
Knoxville, TN 37996

<sup>2</sup>Oak Ridge National Laboratory  
1 Bethel Valley Road  
P.O. Box 2008  
Oak Ridge, TN 37831-6392

E-mail: fcurtis@utk.edu · E-mail: ekici@utk.edu · E-mail: freelsjd@ornl.gov

ing the past half century, significant effort has been made to determine the deflections caused by the coolant flow in the reactor. These analyses were based on the conservative Miller Critical Velocity ( $M_c$ ) [1]. The effectiveness of the  $M_c$  has been argued both analytically by Swinson [2] and Wick [3] and experimentally by Smissaert [4]. A fully numerical approach to the FSI phenomena has not been simulated for the HFIR fuel plates for either the HEU or LEU fuel.

The conversion to LEU fuel is not only planned for the HFIR but across all US research reactors and thus experimental and numerical analyses are being performed to aid in the conversion process. A generic test plate experiment is being designed and constructed at the Oregon State University (OSU) that uses a flat plate, multi-channel design to measure both static and dynamic fuel plate deflections. The experiments performed by OSU and others will be used to validate COMSOL's FSI module and provide confidence for the numerical analysis of the HFIR involute fuel plates. A three-step process has been created for the analysis:

1. Verify the COMSOL FSI module with a simple 2-D and 3-D analysis of a cylinder in cross-flow
2. Create a 3-D plate model that will compare to established (Smissaert) and future (OSU) experimental data
3. And create a 3-D involute geometry effective in predicting the deflection characteristics of both the current HEU fuel and the future LEU fuel.

---

## 2 Governing Equations

The flow field for both the cylinder in cross-flow and the fuel plates is considered to be incompressible. The best representation of the flow is given by the Navier-Stokes (N-S) equations for non-linear, unsteady flow. The derivation is well documented in the literature. In differential form, the N-S equations for laminar flow are given by:

$$\rho \frac{D\mathbf{u}}{Dt} = -\nabla p + \mu \nabla^2 \mathbf{u} + \mathbf{F} \quad (1)$$

and

$$\nabla \cdot \mathbf{u} = 0 \quad (2)$$

where Eq. (1) is the conservation of momentum and Eq. (2) is the conservation of mass. The Reynolds-Averaged Navier-Stokes (RANS) is used for the turbulence models in the COMSOL code. The turbulence models used for our experiments are the  $k - \varepsilon$  model and Low-Reynolds Number (LRN)  $k - \varepsilon$  model.

### 3 Methods

#### 3.1 Cylinder in Cross-flow

To gain confidence in COMSOL's FSI capabilities, the fundamental problem of a cylinder in cross-flow was considered. Previous research has shown that at relatively small Reynolds numbers ( $47 < Re < 180$ ), a phenomenon known as Von Karman vortex shedding occurs in which a vortex is shed alternatively from the top and bottom of the cylinder (Roshko [5] and Williamson [6]). The nature of the shedding is determined solely from the non-dimensional  $Re$  and has a relationship to the Strouhal number ( $St$ ), which is the dimensionless cylinder shedding frequency. The Reynolds number is defined by

$$Re = \frac{U_\infty D}{\nu_\infty} \quad (3)$$

where  $U_\infty$  is the free-stream velocity,  $D$  is the characteristic length of the cylinder (the diameter) and  $\nu_\infty$  is the free-stream kinematic viscosity. The non-dimensional Strouhal number is defined by

$$St = \frac{fD}{U_\infty} \quad (4)$$

where  $f$  is the shedding frequency,  $D$  is the characteristic length and  $U_\infty$  is the free stream velocity.

The cylinder in cross-flow was analyzed for three different cases in 2-D:

1. A stationary cylinder
2. A moving cylinder subject to prescribed motion
3. A moving cylinder modeled as a mass-damper system with the forcing function calculated from the lift created by the shedding vortices

All cases had the same inlet and exit conditions and computational domain. The working fluid was taken to be water, the cylinder diameter was taken to be 1mm, and the inlet velocity varied depending upon the desired Reynolds number. The computational domain is shown in Fig. 1.

Case 1 was run for  $Re = 100$ . In order to cut down computational time, a stationary solution was used as the initial condition for the transient solver. Initial time-accurate runs proved difficult as the cylinder did not exhibit vortex shedding. Upon further inspection, it was discovered that the COMSOL implicit solver, by default, uses an algorithm to determine the minimum time step based upon the instability of the solution. This algorithm did not detect the flow instability and thus created time steps too large to capture the flow phenomena. To alleviate this problem, the

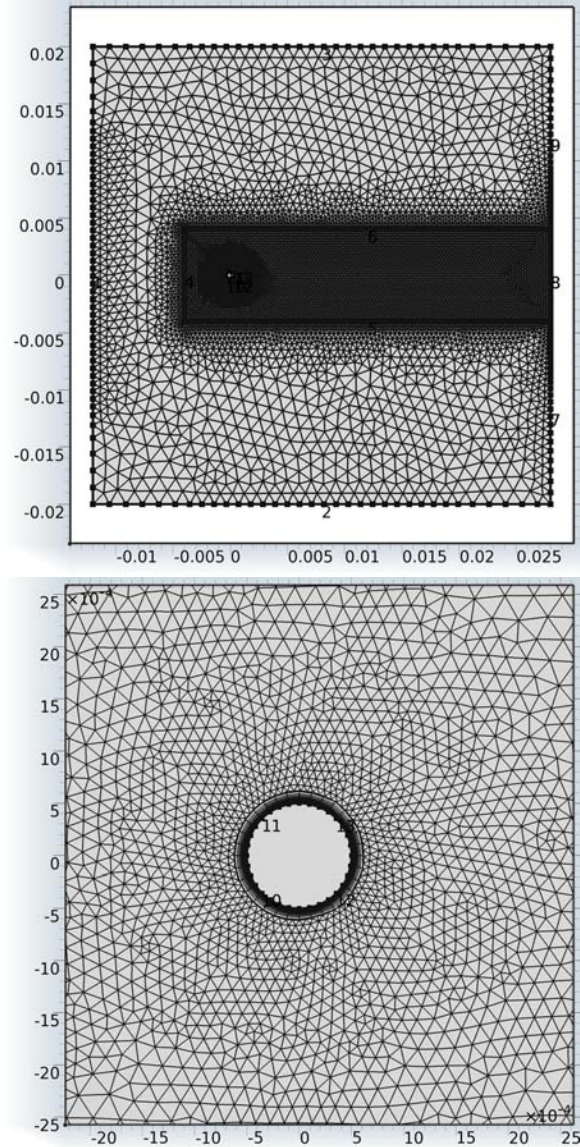


**Fig. 1** The 2-D domain used for the cylinder in cross-flow. The meshing was more dense behind the cylinder in an effort to capture the vortex shedding (top). A close up of the boundary layer mesh around the cylinder (bottom).

maximum time step was limited to 1/10 of the expected shedding frequency for the entirety of the computational run. Although this significantly slowed the computational time, the solution exhibited the expected frequency shedding results.

Case 2 involved a cylinder that was forced to move in plunging motion at a prescribed frequency. For a cylinder that is forced at a frequency near its natural shedding frequency, the shedding frequency will “lock-in” to the oscillating frequency. For forced oscillations outside of this region, the cylinder will shed vortices near the predicted shedding frequency given by the Strouhal number [7]. A representation of the “lock-in” region is provided in Fig. 2.

The forced oscillations were obtained by incorporating the Moving Mesh module and forcing the boundary around the cylinder to oscillate vertically at prescribed frequencies. This helped to demonstrate the arbitrary Lagrangian-Eulerian (ALE) module used for the moving mesh.

Case 3 allowed the cylinder to oscillate based upon the lift induced by the shedding of the vortices. The lift was calculated by integrating the pressure around the cylinder. The movement of the cylinder was established by modeling the cylinder as a mass-damper system and the lift is the forcing function. A mass-damper system is modeled by the following ordinary differential equation (ODE)

$$\ddot{x} + 2\zeta\omega_n\dot{x} + \omega_n^2x = f(t) \quad (5)$$

where  $\zeta$  is the damping ratio,  $\omega_n$  is the natural frequency and  $f(t)$  is the forcing function (lift). This equation was solved by the ODE module in COMSOL and the displacements ( $x$ ) were fed into the ALE module. This created a fully-coupled, 2-D FSI model in COMSOL.

After completing the 2-D moving cylinder, a 3-D model was created and the FSI module was used. All conditions used in the 2-D model were the same except for the natural frequency and damping ratio of the cylinder. This was determined by the length and material properties of the cylinder. The FSI results were compared with those obtained from the 2-D analysis.

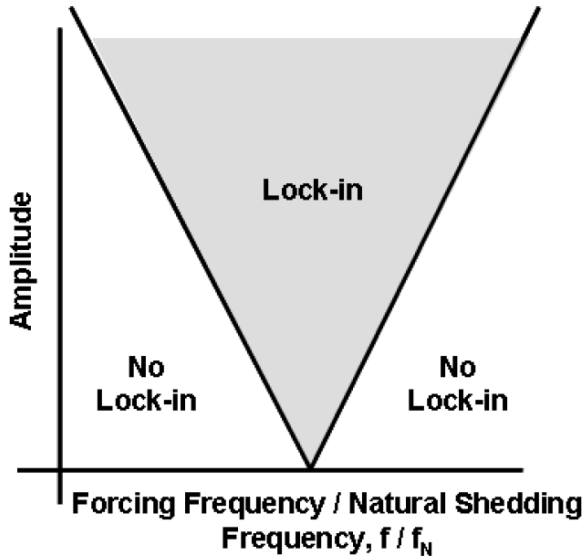


Fig. 2 Representation of the “lock-in” region for a cylinder in cross-flow [7]

### 3.2 3-D Fuel Plate Analysis

Once the cylinder in cross-flow computations were completed, models comparing experimental data available from

Smitsaert and future OSU data could be created and verified. Because data is currently available for Smitsaert’s work, a model was created that represented the experiments performed. The experiments consisted of 5 parallel plates that were 4.5 in wide, 45 in long and approximately 0.06 in thick. A type of PVC plastic was chosen for the plate material by Smitsaert, in order to achieve maximum deflections within the elastic range of the material. In doing this, the data could be compared to  $M_c$  which is defined as

$$M_c = \sqrt{\frac{15Es^3h}{\rho b^4(1-\nu^2)}} \quad (6)$$

where  $E$  is the Modulus of Elasticity,  $s$  is the plate thickness,  $h$  is the height of the channels,  $\rho$  is the fluid density,  $b$  is the width of the plate, and  $\nu$  is the Poisson’s ratio.

Because the flow is in the turbulent regime, a very fine mesh is required along the entire length of the plate in order to resolve the boundary layer. A 2-D analysis was performed to establish the minimum mesh density when going to 3-D flow. Along with deflection data, Smitsaert also provided pressure data within the channels and this data would help determine the necessary meshing along the plates. 3-D analysis is pending verification of the pressure data in 2-D.

## 4 Results

### 4.1 Cylinder in Cross-flow

Case 1 - Once the implicit time-stepping requirements were determined, the cylinder in cross-flow exhibited vortex shedding as expected. The contours of the velocity magnitude are provided in Fig. 3.

To determine the frequency of vortex shedding, the coefficient of lift ( $C_L$ ) on the cylinder surface was computed at different time instances over a few periods of excitation. A Fourier transform was then used on the data to determine the fundamental frequency of excitation. The coefficient of lift is given by

$$C_L = \frac{L}{\frac{1}{2}\rho_\infty U_\infty^2 Ds} \quad (7)$$

where  $L$  is the lift,  $\rho_\infty$  is the free stream density,  $U_\infty$  is the free stream velocity,  $D$  is the diameter of the cylinder and  $s$  is the span or length of the cylinder. For Reynolds number of 100, the predicted shedding frequency using Eq. (4) is approximately 16 Hz. The solution found using COMSOL is provided in Fig. 4 and the shedding frequency matches well with the experimental data.

Case 2 - Using the ALE module, coupled with the laminar flow solver, solutions were obtained for various cases showing both “lock-in” and no “lock-in.” Two cases were performed to demonstrate both the possibility of “lock-in” and no “lock-in” using two different forced frequencies. The first frequency of 18.4 Hz was predicted to show

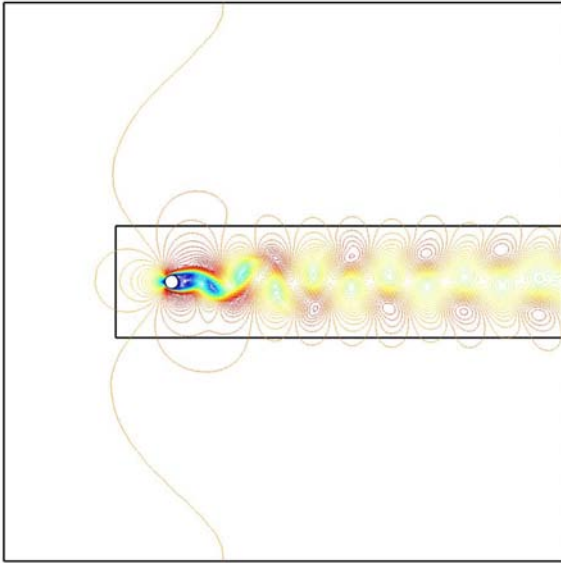


**Fig. 3** Solution of the stationary cylinder in cross-flow.

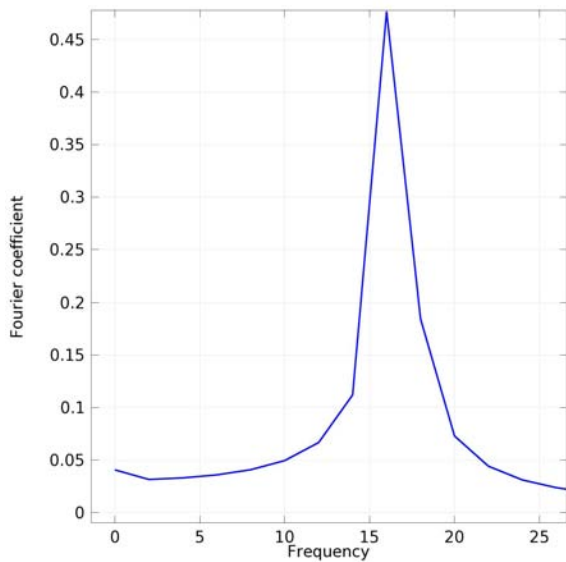


**Fig. 4** Coefficient of lift on the cylinder displayed in the frequency domain using a Fast Fourier Transform (FFT).

“lock-in” and thus the cylinder should shed vortices at only the forcing frequency. The second frequency at 28 Hz should exhibit no “lock-in” and the FFT should show two frequencies, one close to the natural shedding frequency and another one at the forcing frequency. Figs. 5 and 6 demonstrate this concept.

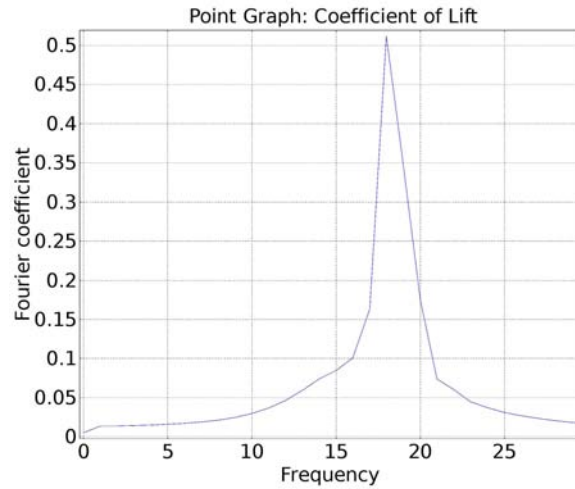


**Fig. 5** The FFT of the  $C_L$  of the cylinder with a forcing frequency of 18.4 Hz demonstrating a case of “lock-in” with only one frequency present.

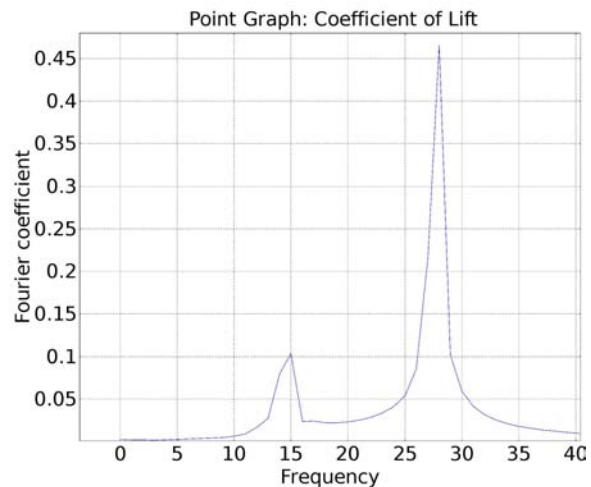


**Fig. 6** The FFT of the  $C_L$  of the cylinder with a forcing frequency of 28 Hz demonstrating a case of no “lock-in” with two distinct frequencies present.

Case 3 - As described in the Methods section, case three allowed the cylinder to freely oscillate based upon the lift created by the shedding of the vortices. The lift around the cylinder was determined and input into the ODE solver of COMSOL for Eq. (5). The result was then fed into the Moving Mesh module which allowed the cylinder to oscillate. This technique simulates a 3-D cylinder in cross-flow. The position of the cylinder as a function of time is provided in Fig. 7

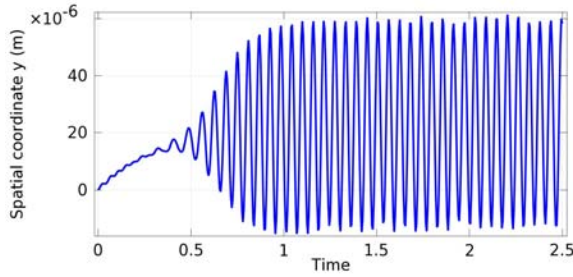


**Fig. 7** The position of the cylinder as a function of time using the lift of the cylinder to drive the movement.

Careful examination of the oscillations of the cylinder will reveal a drift present in the displacement. The cylinder would continually drift and then settle to a new equilibrium position regardless of time stepping or maximum error tolerance. This perplexing phenomena also induced a secondary oscillation observable in Fig. 7. This abnormality was corrected in the 3-D case.

**3-D Cylinder** - The 3-D cylinder in cross-flow used only the FSI module to model the oscillations of the cylinder due to the changes in lift caused by the shedding vortices. It was discovered during this process that the quality of the mesh had a very significant effect in the behavior of the shedding vortices and oscillations of the cylinder. The asymmetry of the mesh, coupled with numerical inaccuracies, caused the flow to be slightly asymmetric resulting in a small, steady lift. To ensure a quality mesh while still using a free-mesh scheme, a horizontal line going through the center of the cylinder was created to ensure an almost symmetric mesh around the cylinder. With this new mesh, the oscillations of the 3-D cylinder exhibited the expected results provided in Fig. 8.

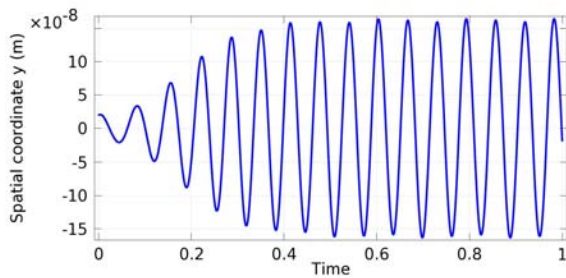


**Fig. 8** The position of the cylinder as a function of time using 3-D FSI.

#### 4.2 3-D Fuel Plate Analysis

As stated in the Methods section, 2-D pressure results will help to determine the correct boundary layer meshing for the 3-D analysis of the fuel plates. Early results for the

PVC plates tested by Smitsaert have shown computational results with an incorrect inlet pressure of approximately 50% difference. Results as compared to experimental data are provided in Fig. 9.

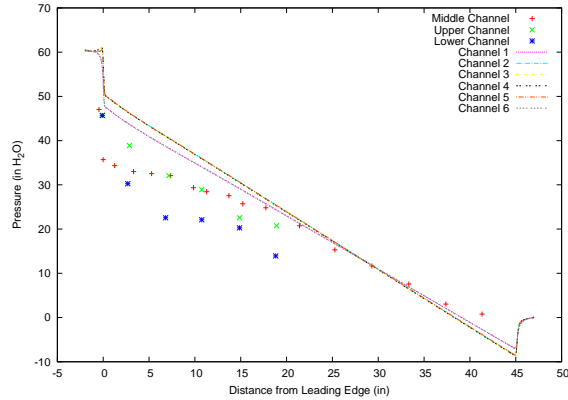


**Fig. 9** Pressure along the length of the channels.

The layout for the computational domain for the 2-D plates is provided in Fig. 10.

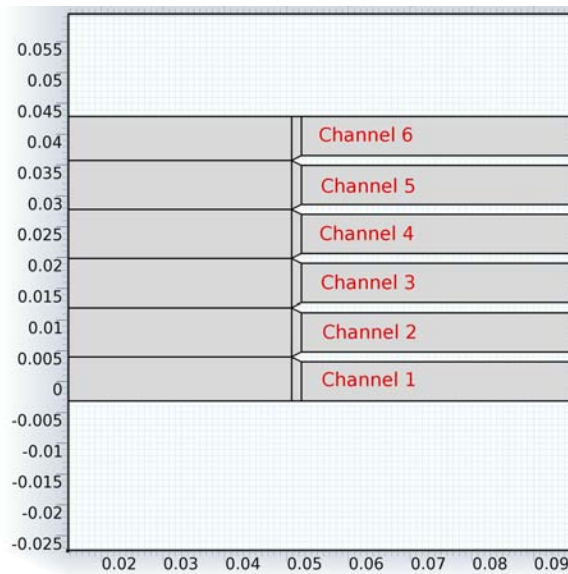


**Fig. 10** The inlet area of the 5 plate domain used for Smitsaert's work.

As seen in Fig. 10, the leading edge of the plates have been sharpened to a point whereas the experimental plates, although not specified, had most likely flat leading edges. If anything, this should decrease the pressure through channels. Interestingly, although the inlet pressure is too high, the pressure along the channel after about 15 in agrees well with the experimental data.

After further inspection of the paper by Smissaert, it has been found that the pressure transducer and inlet flow velocity uncertainties were not specified. Along with other discrepancies in the report, including various plate and channel widths, it is possible that the measurements provided could be slightly off. For the case being used for comparison, Smissaert lists the  $M_C = 8.5 \text{ ft/s}$ , but we calculated the  $M_C = 7.65 \text{ ft/s}$ . A computation was performed to examine the effects of specifying the inlet velocity based on the newly calculated  $M_C$ . Along with the new inlet value, the plate thickness was decreased to 0.05 in and the channel thickness was increased to 0.253 in. The results are provided in Fig. 11.

3. Wick, R. S., "Hydro-elastic Behavior of Multiple-plate Fuel assemblies - I: Pressure Wave Propagation," *Journal of Nuclear Energy*, Vol. 23, 1969, pp. 387–405.
4. Smissaert, G. S., "Static and Dynamic Hydroelastic Instabilities in MTR-type Fuel Elements Part 1. Introduction and Experimental Investigation," *Nuclear Engineering and Design*, Vol. 7, 1968, pp. 535–546.
5. Roshko, A., *On the Development of Turbulent Wakes from Vortex Streets*, Ph.D. thesis, California Institute of Technology, 1952.
6. Williamson, C. H. K., "Defining the Universal and Continuous Strouhal-Reynolds Number Relationship for the Laminar Vortex Shedding of a Circular Cylinder," *Physics of Fluids*, 2004.
7. Spiker, M. A., *Development of an Efficient Design Method for Non-synchronous Vibrations*, Ph.D. thesis, Duke University, 2008.

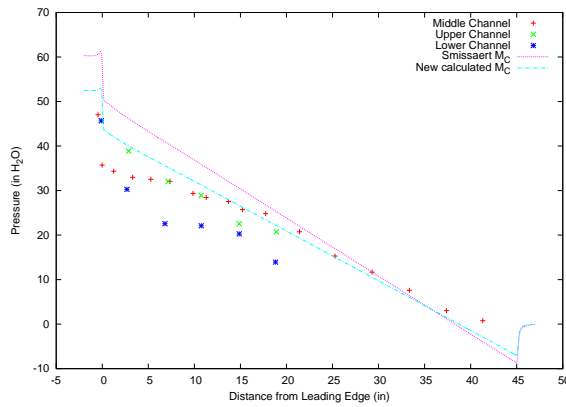


**Fig. 11** Comparison of pressure data for the  $M_C = 8.5 \text{ ft/s}$  (Smissaert's value) and the  $M_C = 7.65 \text{ ft/s}$  (new calculated value).

The results presented in Fig. 11 show that Smissaert may have inaccuracies with the measurements provided. A small change in parameters produces results that better agree with his experimental data. A 3-D model will be run for Smissaert's PVC plate experiment and comparisons will be made.

## 5 Conclusion

The ability of COMSOL to perform multi-physics analysis while allowing the coupling of additional external equations upon input has proven to be a very powerful tool. We will model the OSU test plates and anticipate that the data will validate our approach for COMSOL.

## References

1. Miller, D. R., "Critical Flow Velocities for Collapse of Reactor Parallel-Plate Fuel Assemblies," Tech. Rep. KAPL-1954, Knolls Atomic Power Lab, 1960.
2. Swinson, W. F. and Yahr, G. T., "Dynamic Pressure Approach to Analysis of Reactor Fuel Plate Stability," Tech. Rep. CONF-900608-21, Oak Ridge National Laboratory, 1990.